RSC Advances

A simple donor-acceptor probe for detection of Cr3+ cations

Journal:	*RSC Advances*
Manuscript ID:	RA-ART-01-2014-000034.R1
Article Type:	Paper
Date Submitted by the Author:	04-Feb-2014
Complete List of Authors:	Xu, Yunlong; Soochow University, School of Chemistry & Chemical Engineering and Material Science yang, wen; soochow university, Shao, Jie; Soochow University, zhou, weiqun; soochow university, zhu, wei; soochow university, College of Chemistry, Chemical Engineering and material Science Xie, Juan; Soochow University,

A simple donor-acceptor probe for detection of Cr^{3+} cations

Yunlong Xu , Wen Yang, Jie Shao, Weiqun Zhou*, Wei Zhu, Juan Xie

School of Chemistry & Chemical Engineering and Material Science, Soochow University, 199 *Ren'ai Road*, *Suzhou*, *People's Republic of China*, *215123*

Abstract

A simple probe (**1**, 1-(4-cyano-phenyl)-3-(4-dimethylamino- phenyl)-thiourea)) as a ligand for metal ions is prepared and characterized by elemental analysis, nuclear magnetic resonance ($^{1}H/^{13}C$ NMR), Mass spectra and fourier transform infrared spectrometry (FTIR). The probe exhibits fluorescence enhancement upon exposure to chromium(III) in THF/water (V/V=9/1) buffer solution (trihydroxymethyl aminomethane-hydrochloric acid (Tris-HCl), pH = 7.4). Chelation photo-induced electronic transfer (PET) mechanism was introduced to explain the fluorescence enhancement with high selectivity and sensitivity. It was found that the probe has a detection limit of 8.18×10^{-7} M. Furthermore, fluorescence imaging experiments of the exciplex (**1**@Cr^{3+}) in human glioma living cells (U251) evidenced its practical application potentiality in biological systems.

Keywords: Fluorescence probe, Trivalent chromium, Photo-induced electron transfer, Fluorescence imaging.

* Corresponding author, Tel: 86-0512-65884827
E-mail: wqzhou@suda.edu.cn,
Postal address: Soochow University, 199 Ren'ai Road, Suzhou, P. R. China, 215123

Introduction

Development of chemo-sensors for sensing and recognition of environmentally and biologically important metals such as Cr^{3+} has attracted considerable attention from current researchers [1-3]. The release of aqueous chromium to the nature at numerous ways through a variety of industrial processes such as metallurgical, chemical industries, electroplating and so on[4]. As an environmental contaminant, chromium is found mostly in Cr^{6+} form and its bacterial reduction to Cr^{3+} is considered as one of the promising strategies for bioremediation [5-6]. Cr^{3+} has also recently shown to adversely affect cellular structures, although its in vivo toxicity is observed to be lower than that of Cr^{6+} [7].

Generally, traditional analytical techniques such as atomic absorption/emission spectroscopy or inductively coupled plasma mass spectrometry are costly and time-consuming which makes them not suitable for fast and convenient detection of the ion analytes. In contrast, the fluorescent probes adopted for sensing of a specific analyte are very popular for achieving higher sensitivity, rapid and reversible detection, and possible application in imaging studies for diagnostic applications.

Nowadays, a large number of chemosensors for metal cations have been shown in the literatures. However, very few studies have been devoted to the development of organic probes that are sensitive to Cr^{3+} which can turn-on the fluorescence, because of the paramagnetic nature of Cr^{3+} for fluorescence quenching of fluorophore via enhancement of spin–orbit coupling [8-11]. Moreover, the reported sensors [12-14] were relative to a complicated preparation process. Therefore, the development of sensitive, selective, reversible chemosensors for Cr^{3+} in various media is significant.

Thiourea moiety is a strong hydrogen bond donor and is widely used in design and preparation of anion sensors as anion binding sites [15-18]. The thiourea group is also an excellent ligand, which can strongly bind metal ions [19-21]. In this paper, we synthesized a simple probe with thiourea moiety as binding sites for Cr^{3+}. The probe **1** could be easily prepared at room temperature. The probe **1** exhibited turn-on fluorescence responses to Cr^{3+} in THF/water (V/V=9/1)

buffer solution (Tris-HCl, pH = 7.4). To the best of our knowledge, such simple probe based on thiourea derivative for detection of Cr^{3+} is first reported.

Experimental

Chemicals and reagents

THF, TDF-*d8* were used as HPLC grade purchased from *J&K* (CHINA). Metal ions were provided from $CaCl_2$, $CdCl_2$•$5H_2O$, $CoCl_2$•$6H_2O$, $CrCl_3$, $CuCl_2$•$2H_2O$, $FeCl_3$, $HgCl_2$, KCl, $MgSO_4$, $MnCl_2$, NaCl, $NiCl_2$, $PbCl_2$ and $Zn(NO_3)_2$ as HPLC grade reagents purchased from COSMOSIL (CHINA). Two stock solvents were prepared showing the following proportions: THF/water (V/V=9/1) Tris–HCl buffer (10 mM, pH = 7.4) solution and THF/water (V/V=1/9) Tris–HCl buffer (10 mM, pH = 7.4) solution. Melting points were determined on a Kofler melting point apparatus and uncorrected. IR spectra were obtained in KBr pellets using a Nicolet 170SX FT-IR spectrometer. ^{1}H NMR and ^{13}C NMR spectra have been recorded on INOVA 400 at 400 and 100 MHz, respectively, usings ppm. Elementa TMS as internal standard and TDF-*d8* as deuterated solvents with chemical shifts reported al analyses were performed on a Yannaco CHNSO Corder MT-3 analyzer. Absorption and fluorescence spectra were recorded by using a CARY50 UV-VIS spectrophotometer and an FLS920 fluorescence spectrophotometer, respectively. Mass spectra was recorded on Finnigan MAT95 mass spectrometer (ESI^+). The fluorescence quantum yield was evaluated by using quinine sulfate in 0.05 mol•L^{-1} (0.05 M) sulfuric acid as the standard. All the experiments were carried out at room temperature. All of the images were gathered at the same Live Cell Imaging System (Olympus, Cell'R) and processed with Nikon AY software.

*Synthesis of the probe **1***

The synthetic route of the probe **1** is depicted in Scheme 1. To the solution of phenylisothiocyante (1) (5.0 g) prepared according to the reported method [22] in acetonitrile (10 mL), *p*-cyano aniline containing electron-withdraw functionality (2) (equal molar ratio) was added and then the resulting mixture was stirred for 3–4 h at room temperature and then evaporated under reduced pressure. The solid was washed by alcohol (10mL, twice) and dried over Na_2SO_4. The composition and structure were determined by elemental analysis, ^{1}H NMR, ^{13}C NMR, IR and HRMS. Yield: 45.5%. m.p.: 153.4 □. Anal. Calc. formula, $C_{16}H_{16}N_4S$, (%): C, 64.86; N, 18.92; H, 5.41. Found (%): C, 64.95; N,18.83; H, 5.43. ^{1}H NMR (δ, ppm, Figure S1): 2.868(s, 6H,

2CH_3), 6.692- 6.717(d, 2H, J=8.8 Hz), 7.222-7.199 (d, J=8.8 Hz, 2H), 7.752 (s, 4H), 9.163(s, 1H), 9.922(s, 1H). ^{13}C NMR (ppm, Figure S2): δ: 179.328(1C, C-S), 149.554(1C, ph), 146.314(1C, ph), 142.546(1C, ph), 132.482(1C, ph), 127.235(1C, ph), 123.253(1C, ph), 118.640(1C, CN), 112.760(1C, ph), 108.022(1C, ph), 40.379(2C, CH_3). FTIR (ν, cm^{-1}, Figure S3): 3466(νN1H1), 3263(νN2H2), 3043(νPh-H), 2871(νPh-H), 2871.5(νCH_3, as), 2824(νCH_3, s), 2396(νS-H), 2229(νC≡N), 1617(νPh), 1599(νC=C), 1532(νN-C-N, as), 1444(νCN), 1404(νCN), 1346(νPhN), 1264(νC-S), 1233(νCN), 1186(νCN), 1166(δCCH), 1152(δCCH), 1114(νCC), 1072(νCN), 1015(νCN), 943(γCH), 867(τC-N), 828(γCH), 781(γCH),748(νCS), 687.9(γCH). HRMS (ESI, Figure S4) calcd. for $(M+H^+)^+$ 297.1, found 297.1.

Scheme 1

The pH dependence, the binding stoichiometry, the association constants and the detection limit

The probe **1** (20 μM) was added with Cr^{3+} in different pH THF/water (9/1) solution. The binding stoichiometry of **1**@Cr^{3+} was determined from a Job plot [23]. The fluorescence intensity at 467 nm was plotted against the molar fraction of the probe with 0-2.0 equivalents of Cr^{3+}. The association constant (K_a) of **1**@Cr^{3+} is determined by the Benesi–Hildebrand Eq. (1) [24]:

$$\frac{1}{F-F_0}=\frac{1}{\{K_a\times(F_{\max}-F_0)\times[Cr^{3+}]\}}+\frac{1}{F_{\max}-F_0} \quad (1)$$

Where F is the fluorescence intensity at 467 nm at any given Cr^{3+} concentration, F0 is the fluorescence intensity in the absence of Cr^{3+}, and Fmax is the maxima fluorescence intensity at 467 nm in the presence of Cr^{3+} in solution. The association constant K_a was evaluated graphically by plotting 1/ ($F-F_0$) against 1/ [Cr^{3+}]. Data were linearly fitted according to Eq. (1) and the K_a value was obtained from the slope and intercept of the line. The detection limit (DL) of Cr^{3+} was determined from the following equation: DL = K × SD/S [25], where K = 3, SD is the standard deviation of the blank solution, and S is the slope of the calibration curve.

Cell culture and fluorescence imaging

U251 cells were purchased from the Shanghai Institute of Cell Biology. The cells were cultured in Roswell Park Memorial Institute culture medium (RPMI-1640), supplemented with 6% calf serum, penicillin (100 $U\cdot mL^{-1}$), streptomycin (100 $\times10^{-6}$ $g\cdot mL^{-1}$) and 2.5 × 10^{-4} M l-glutamine at 37℃ in a 5:95 CO_2–air incubator. The cells were cultured in a 15 mm diameter cell culture dish

for 2 days. U251 cells were incubated with a solution of **1** (20 μM, THF/water = 1/9, V/V, pH=7.4, tris-HCl buffer solution) for 0.5 h, then the dish was subjected to long-term imaging using a living cell imaging system (Olympus, Cell'R) equipped with an objective lens (Olympus, UAPO 40×/340 N.A. = 0.90), a halogen lamp, a red LED (620 nm). The emission was collected at 480 nm (λ_{ex}=340 nm). Then, further treated with Cr^{3+} (40 μM, THF/water = 1/9, V/V, pH=7.4, tris-HCl buffer solution) for 30 min in the culture medium, and washed with PBS buffer to remove extracellular. The images were obtained every 10 min for the indicated time courses.

Results and discussion

The turn on fluorescence to recognize Cr^{3+} recognition

The fluorescent property of the probe **1** was investigated in THF/water (9/1, V/V) in Tris-HCl buffer solution (pH=7.4) under excitation at 350 nm. The weak fluorescence band at λ_{max} = 467 nm (Stocks shift = 117 nm) is observed in Figure 1(a) and it can be assigned to a charge transfer (CT, MLCT) band transition [26-30]. The fluorescence quantum yield was evaluated as being 0.042. The fluorescence recognition properties of the probe **1** were further investigated upon the excitation at 350 nm in THF/H_2O (9/1, pH=7.4) buffer solution. Figure 1(a) shows fluorescence responses of the probe **1** (20 μM) to different metal ions (40 μM). Obviously, the fluorescence intensity enhancement was only observed when Cr^{3+} was added to the probe **1** solution, whereas, the addition of the other cations did not cause any increase in the fluorescent emission intensity. When the concentration of Cr^{3+} increased to 0.5 equiv. (10 μM), the fluorescence enhancement factor (($F- F_0$)/F_0) reached to 22.2 (see Figure 1(b)). The Job plots further proved the formation of a **1**@Cr^{3+} complex with 2:1 stoichiometry in solution (see Figure 1(c)).

Figure 1

Absorption titration study

The UV-Vis spectrum of the probe, viewed in Fig. 2, shows the characteristic absorption bands with maximum at 271 nm and 306 nm assigned to intramolecular n–π* transitions. In UV-Vis titration, after the addition of Cr^{3+} ion solution to the probe **1** solution (20 μM, THF/water = 1/9, V/V, pH=7.4, tris-HCl buffer solution), it can be observed a new band with maximum at 344 nm. The band in the UV region at 306 nm observed in the absorption spectrum of the probe **1**, gradually decreases its intensity with the addition of Cr^{3+} ions and simultaneously a new band

appears at 344 nm and starts to increase with a 38 nm red shift through an isosbestic point at 320 nm (Fig. 2) due to the formation of the Cr^{3+} complex with the probe.

Figure 2

The competition

The competition experiment of the metal ions exhibited minor influences on Cr^{3+} induced fluorescence intensity of the probe except for Ag^{+}, Cu^{2+}, Fe^{3+} and Hg^{2+}, which can result in the fluorescence quenching in some degree (Figure 3). In the coexistence of Cr^{3+} and Ag^{+}, Cu^{2+}, Fe^{3+} and Hg^{2+}, the enhancement factor $((F- F_0)/F_0)$ of the probe reduced to 10.2 (Ag^{+}), 10.0 (Cu^{2+}) ,8.8 (Fe^{3+}) and 10.9 (Hg^{2+}) (see Figure 3). As we known, Ag^{+}, Cu^{2+} and Hg^{2+} can coordinated to S atom of thiourea, which resulted in a fluorescence quenching. Obviously, the coordination with Ag^{+}, Cu^{2+} and Hg^{2+} was weaker than the chelation of Cr^{3+} with N of thiourea. So, the coexistence of 1@Cr^{3+} complex and Ag^{+}, Cu^{2+} , Fe^{3+} or Hg^{2+} cations lead to a small decrease of the enhancement factor $((F-F_0)/F_0)$ that does not cause a considerable interference in the Cr^{3+} detection by the probe **1**.

Figure 3

The range of pH

A pH titration of the probe was conducted to investigate in a suitable pH range THF/water (9/1) solution for Cr^{3+} sensing. Figure 4(a) shows that the changes of the fluorescence enhancement $(F-F_0)$ of **1**@Cr^{3+} were small at a pH range of 6~8. The fluorescence intensity decreased dramatically when the pH value is lower than 6, which can be attributed to the protonation of thiocarbony group of the probe that blocked the formation of the **1**@Cr^{3+} complex. When the pH value is higher than 8, the decrease of fluorescence is a consequence of the hydrolyzation of Cr^{3+} that inhibited the formation of 1@Cr^{3+} complex. Thus the best pH range considered for Cr^{3+} sensing is approximately 6 to 8.

The association constant K_a of **1**@Cr^{3+} is described in Figure 4(b). The fitted Benesi–Hildebrand equation was linearized and the obtained association constant K_a for Cr^{3+} binding to the probe was $5.56\times10^{4}\ M^{-1}$. The detection limit of the probe was determined from the plot of fluorescence intensity as a function of the concentration of Cr^{3+} (see Figure 4 (c)). It was found that the probe has a detection limit of 8.18×10^{-7} M (SD=24.3, n=12) for Cr^{3+}.

Figure 4

Fluorescence recognition mechanism

It is well known that Cr^{3+} can quench the fluorescence of a fluorophore because of its paramagnetic property. But the fluorescence enhancement responses are preferred for designing efficient sensors. The enhanced fluorescence response binding Cr^{3+} could be attributed to the block of photo-induced electron transfer (PET). The mechanism of the enhanced fluorescence response is depicted in Scheme 2. According to the introduction of Bernard Valeur, when the amino group strongly interacts with a cation, the electron transfer is hindered and a very large enhancement of fluorescence is observed. Upon excitation of the fluorophore, an electron of the highest occupied molecular orbital (HOMO) is promoted to the lowest unoccupied molecular orbital (LUMO), which enables PET from the HOMO of the donor (cation-free receptor) to that of the fluorophore, causing fluorescence quenching of the latter. Upon cation binding, the redox potential of the donor is raised so that the relevant HOMO becomes lower in energy than that of the fluorophore, PET is no longer possible and the electron of fluorophore which is in the excited state can return to ground state leading to the fluorescence enhancement as a consequence [31].

Scheme 2

Living cell imaging

To detect Cr^{3+} in living cells, U251 cells were cultured in RPMI-1640 supplemented with 6% FBS at 37°C and 5% CO_2. Cells were plated on 15 mm culture dish and allowed to adhere for 48 h. Upon incubation with 20 μM (THF/water=1/9, V/V, pH=7.4 Tris-HCl buffer solution) of the probe **1** for 30 min at 37°C, the cells displayed a weak intracellular blue fluorescence image. When further treated with $CrCl_3$ (40 μM, THF/water=1/9, V/V, pH=7.4 Tris-HCl buffer solution) for 10 min in the culture medium, and washed with PBS buffer to remove extracellular Cr^{3+}, the blue fluorescence enhanced gradually. The fluorescence images are depicted in Figure 5. The fluorescence and bright-field images revealed that the fluorescence signals were localized in the perinuclear area of the cytosol, indicative of a subcellular distribution due to the high cell membrane permeability of the probe **1** [32]. These results demonstrated that the probe **1** was cell membrane permeable and can also be used for imaging of Cr^{3+} in living cells and potentially in vivo.

Figure 5

Conclusions

We successfully developed a simple probe based on 1-(4-cyano-phenyl)-3-(4-dimethylamino-phenyl)-thiourea for detection of Cr^{3+}. The probe **1** also exhibited turn-on fluorescence responses to Cr^{3+} at in THF/water buffer solution. Such fluorescence enhancement with high selectivity and sensitivity was attributed to the inhibition of PET. It was found that the probe has a detection limit of 8.18×10^{-7} M. Furthermore, the probe **1** showed good cell-permeable and distinct blue fluorescence in U251 living cell. It is successfully applied to determine Cr^{3+} in U251 living cells, which demonstrated its value of practical application in the physiological system.

Acknowledgments

This work was supported by the National Natural Science Foundation of China (No. 51079094) and the Natural Science Foundation of Jiangsu Province (No. BK2010215).

References

[1] K. W. Huang, H. Yang, Z. G. Zhou, M. X. Yu, F. Y. Li, X. Gao, T. Yi, C. H. Huang, 2008, Org Lett 10: 2557-60.

[2] P. Mahato, S. Saha, E. Suresh, R. Di Liddo, P. P. Parnigotto, M. T. Conconi, M. K. Kesharwani, B. Ganguly, A. Das, 2012, Inorg Chem 51: 1769-77.

[3] H. M. Wu, P. Zhou, J. Wang, L. Zhao, C.Y. Duan, 2009, New J Chem 33: 653-8.

[4]. M. Manjira, S. Buddhadeb, P. Siddhartha, S. H. Maninder, K. M. Sushil, R. K. B. Anisur and C. Pabitra, 2013, RSC Adv., 3:19978–19984

[5] D. J. Lovley, 1995, Ind Microbiol 14: 85-93.

[6] H. Arakawa, R. Ahmad, M. Naoui, H. A. Tajmir-Riahi, 2000, J Biol Chem 275: 10150-3.

[7] R. Bencheikh-Latmani, A. Obraztsova, M. R. Mackey, M. H. Ellisman, B. M. Tebo, 2007, Environ Sci Technol 41: 214-20.

[8] M. Sarkar, S. Banthia and A. Samanta, Tetrahedron Lett., 2006, 47, 7575.

[9] J. Mao, L. Wang, W. Dou, X. Tang, Y. Yan and W. Liu, Org. Lett., 2007, 9, 3187

[10] H. Wu, P. Zhou, J. Wang, L. Zhao and C. Duan, New J. Chem., 2009, 33, 653.

[11] S. Guha, S. Lohar, A. Banerjee, A. Sahana, I. Hauli, S. K. Mukherjee, J. S. Matalobos and D. Das, Talanta, 2012, 91, 18.

[12] A. Tunceli and A. R. Turker, Talanta, 2002, 57, 1199.

[13] R. K. Sharma and A. Goel, Anal. Chim. Acta, 2005, 534,137

[14] L. Lin, N. S. Lawrence, S. Thongngamdee, J. Wang and Y. Lin, Talanta, 2005, 65, 144.

[15] A. Vargas Jentzsch, A. Hennig, J. Mareda, S. Matile, 2013, Acc Chem Res ; in press.

[16] R. M. Duke, T. McCabe, W. Schmitt, T. Gunnlaugsson, 2012, J Org Chem 77: 3115-26.

[17] A. J. Lowe, B. M. Long, F. M. Pfeffer, 2013, Chem Commun 49: 3376-88.

[18] Z. H. Liu, S. Devaraj, C.R. Yang, Y.P. Yen, 2012, Sens Actuators B 174: 555-62.

[19] Z. P. Liu, W. J. He, Z. J. Guo, 2013, Chem Soc Rev 42: 1568-1600.

[20] M. Vonlanthen, N. S. Finney, 2013, J Org Chem 78: 3980-8.

[21] G. Sanchez, D. Curiel, I. Ratera, A. Tarraga, J. Veciana, Molina, 2013, P Dalton Trans 42: 6318-26.

[22] N. B. Ambati, V. Anand, P. Hanumanthu, 1997, Synth Commun 27: 1487-93.

[23] A. Senthilvelan, I. Ho, K. Chang, G. Lee, Y. Liu, W. Chung, 2009, Chem Eur J 15: 6152–60.

[24] (a) A. Mallick and N. Chattopadhyay, Photochem. Photobiol., 2005, 81, 419; (b) H. A. Benesi and J. H. Hildebrand, J. Am.Chem. Soc., 1949, 71, 2703.

[25] S. R. Liu, S. P. Wu, 2012, Sens Actuators B Chem. 171-172: 1110-6.

[26] W. Yang, W. Q. Zhou, Z. J. Zhang, 2007, J Mol Struct 828: 46–53.

[27] G. Q. Tang, J. MacInnis, M. Kasha, 1987, J Am Chem Soc 109: 2531-3.

[28] J. Heldt, D. Gormin, M. Kasha, 1988, Chem Phys Lett 150: 433-6.

[29] J. Heldt, D. Gormin, M. Kasha, 1988, J. Am. Chem. Soc. 110: 8255-6.

[30] J. Heldt, D. Gormin, M. Kasha, 1989, Chem Phys 136: 321-34.

[31] V. Bernard , 2001, Wiley-VCH Verlag GmbH.

[32] J. Cao, C. C. Zhao, X. Z. Wang, Y. F. Zhang, W. H. Zhu, 2012, Chem Comm. 48: 9897-9.

Figure captions

Scheme 1 The synthetic route of the probe **1**.

Scheme 2 The proposed recognition mechanism by probe **1** for Cr^{3+}.

Figure 1 Fluorescence changes of the probe **1** (20 μM) upon addition of different metal ions (40 μM) (a), fluorescence intensity of the probe **1** (20 μM) upon addition of different equiv. Cr^{3+} ion (b), the stoichiometry analysis of **1**@Cr^{3+} by Job's plot analysis (c) in THF/water buffer solution (λ_{ex} = 350 nm).

Figure 2 Absorption of the probe **1** (20 μM) upon addition of different equiv. Cr^{3+} ion

Figure 3 The fluorescence competitions of probe **1** (20 μM) between Cr^{3+} and the other ions (40 μM) in THF/water buffer solution (λ_{ex} = 350 nm).

Figure 4 The fluorescence enhancement of **1** (20 μM) after adding 2.0 equivalents Cr^{3+} in different pH values aqueous solution (a), the association constant K_a of **1**@Cr^{3+} (b) and the detection limit of the probe **1** for Cr^{3+} (c).

Figure 5 Fluorescence images of U251 cells treated with **1** and KI. (a) Bright field image, (b) fluorescence image loaded with 20 μM probe **1** for 30 min and (c) fluorescence image of **1** loading cells incubated with 40 μM Cr^{3+} for 30 min.

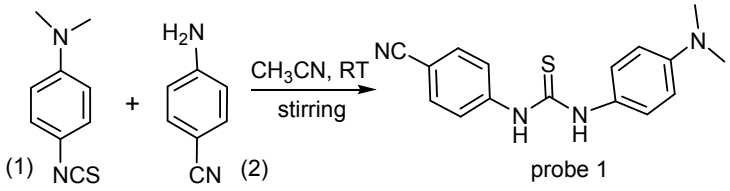

Scheme 1 The synthetic route of the probe **1**.

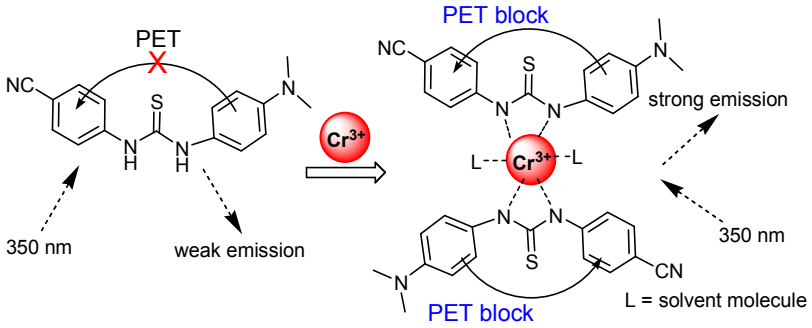

Scheme 2 The proposed recognized mechanism for Cr^{3+}.

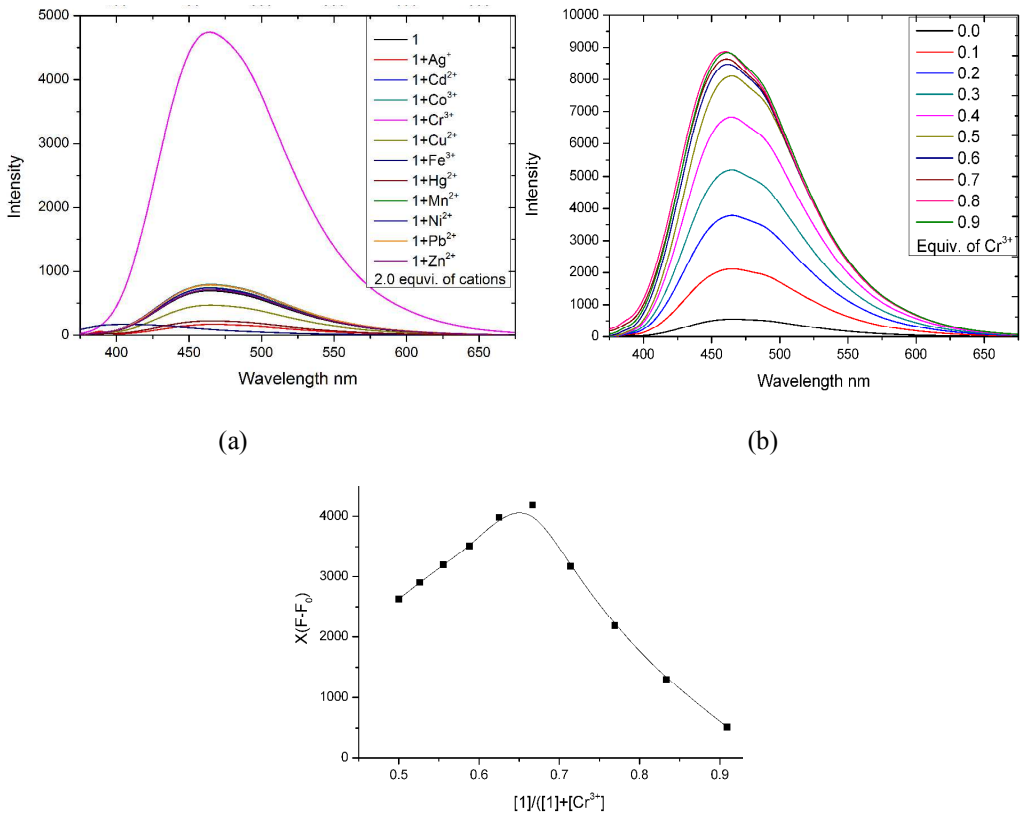

(a) (b)

(c)

Figure 1 Fluorescence changes of the probe **1** (20 μM) upon addition of different metal ions (40 μM) (a), fluorescence intensity of the probe **1** (20 μM) upon addition of different equiv. Cr^{3+} ion (b), the stoichiometry analysis of **1**@Cr^{3+} by Job's plot analysis (c) in THF/water buffer solution.

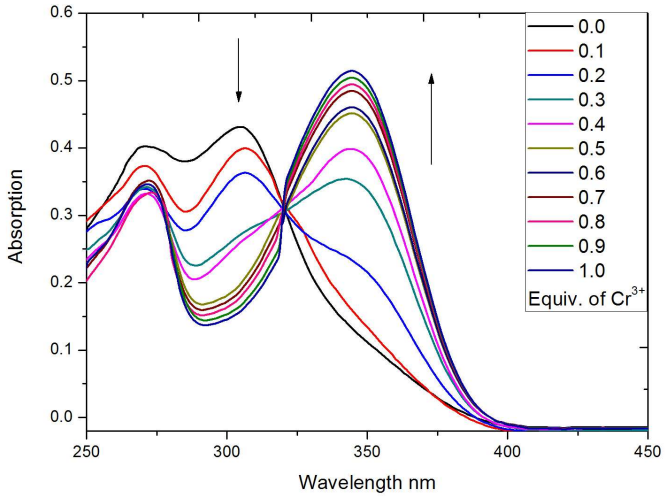

Figure 2 Absorption of the probe **1** (20 μM) upon addition of different equiv. Cr^{3+} ion

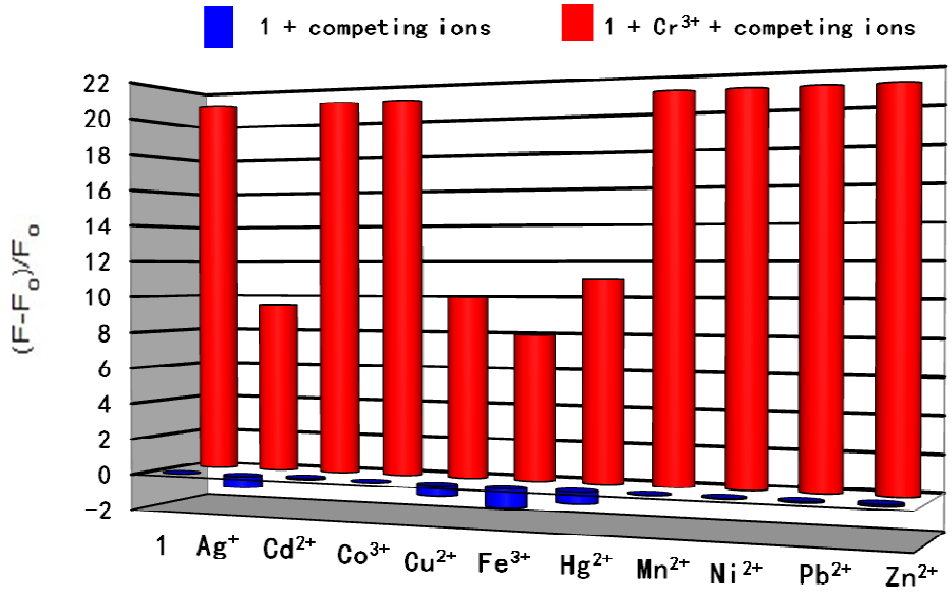

Figure 3 The fluorescence competitions of probe **1** (20 μM) between Cr^{3+} and the other ions (40 μM) in THF/water buffer solution.

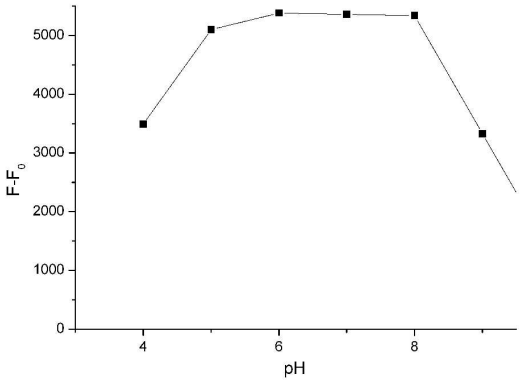

(a)

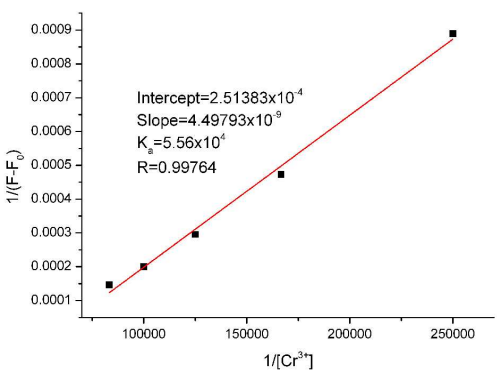

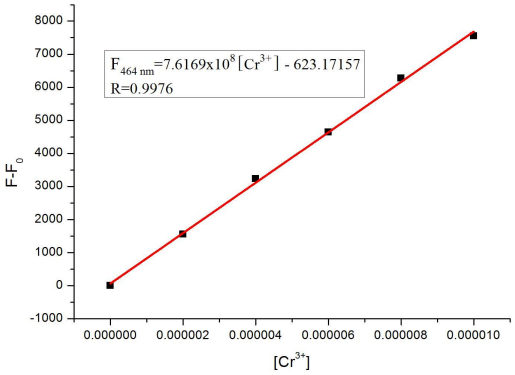

(b) (c)

Figure 4 The fluorescence enhancement of **1** (20 μM) after adding 2.0 equivalents Cr^{3+} in different pH values aqueous solution (a), the association constant K_a of **1**@Cr^{3+} (b) and the detection limit of the probe **1** for Cr^{3+} (c).

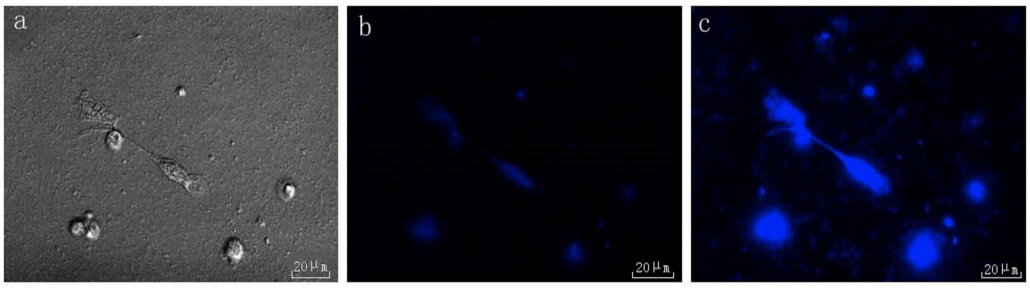

Figure 5 Fluorescence images of U251 cells treated with **1** and KI. (a) Bright field image, (b) fluorescence image loaded with 20 μM probe **1** for 30 min and (c) fluorescence image of **1** loading cells incubated with 40 μM Cr^{3+} for 30 min.

Graphical Abstract

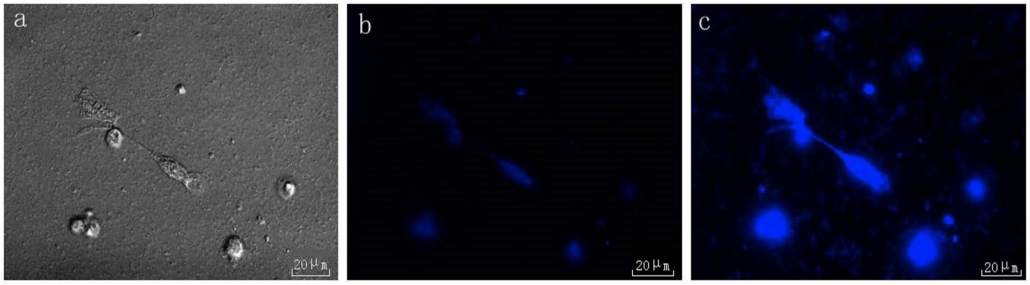

Fluorescence images of U251 cells treated with **1** and KI. (a) Bright field image, (b) fluorescence image loaded with 20μM probe **1** for 30 min and (c) fluorescence image of **1** loading cells incubated with 40μM Cr^{3+} for 30 min.